International Journal of Current Engineering and Technology
ISSN 2277 - 4106

Available at http://inpressco.com/category/ijcet

Research Article

Gold Nanoparticles capped with Tamarind Seed Polysacharide blended with Chitosan composite for the growth of Phosphate Mineral

S.K Biswal[a*],U.K Parida[b] and B.K Bindhani[b]

[a]Department of Chemistry, Centurion University of Technology and Management, Odisha, India
[b]School of Biotechnology, KIIT University, Bhubaneswar, Odisha, India

Accepted 10 August 2013, Available online 20 August 2013, **Vol.3, No.3 (August 2013)**

Abstract

Growth of hydroxyapatite (HA) on Tamarind Seed Polysacharide (TSP)–chitosan composite capped gold nanoparticles is presented for the first time by employing wet precipitation methods and we obtained good yields of HA. Fourier transform infrared spectroscopy (FTIR) spectrum has shown the characteristic bands of phosphate groups in the HA. Scanning electron microscopy (SEM) pictures have shown spherical nanoparticles with the size in the range of 50–150 nm, whereas ≥2–50 nm sized particles were visualized in high resolution transmission electron microscopy (HR-TEM). X-ray diffraction (XRD) spectrum has shown Bragg reflections which are comparable with the HA. Energy dispersive X-ray (EDX) studies have confirmed calcium/phosphate stoichiometric ratio of HA. The thermogravimetric analysis (TGA) has shown about 74% of inorganic crystals in the nanocomposite formed. These results have revealed that TSP–chitosan capped gold nanoparticles, acted as a matrix for the growth of HA.

Keywords*: TSP –chitosan composite, Wet precipitation, Hydroxyapatite , Gold nanoparticles , Nanocomposite materials*

Introduction

Nanoparticles (1–100 nm) have been a source of intense interest due to their novel electrical, optical, physical, chemical, and magnetic properties. They have significant potential for a wide range of applications such as catalysis, magnetic recording media, optoelectronic materials, magnetic fluids, composite materials, fuel cells, pigments, and sensors. Their uniqueness arises from their high ratio of surface area to volume (C. S¨onnichsen *et al*,2002).

Chitosan and its composites have been used in bone tissue engineering (Zhao F *et al*,2002). Chitosan (poly-1, 4, D-glucosamine) a partially de-acetylated derivative from chitin is structurally similar to glycos- aminoglycan (GAG) and has many desirable properties as tissue engineering scaffolds (Suh JKF *et al*,2000). Chitosan finds extensive application due to its low cost, large-scale availability, antimicrobial activity (Khor E *et al*,2003), biodegradability, non-toxicity and its adsorption properties (Dufresne A *et al*,1999). The free amino group in chitosan has chelating, film forming properties and is soluble in 0.3 N acetic acid. The mechanical and the biological properties of chitosan can be increased by blending it with gelatin which has the capacity to form polyelectrolyte complex (Mao JS, Zhao LG *et al*,2003) and has found much attention in bone replacements. The TSP–chitosan network has been found to be safe, haemostatic and osteoinductive and does a good work on drug delivery (Gurpreet Kaur *et al*,2010).

Hydroxylapatite, also called hydroxyapatite (HA), is a naturally occurring mineral form of calcium apatite with the formula $Ca_5(PO_4)_3(OH)$, but is usually written $Ca_{10}(PO_4)_6(OH)_2$ to denote that the crystal unit cell comprises two entities. Hydroxylapatite is the hydroxyl endmember of the complex apatite group. The OH^- ion can be replaced by fluoride, chloride or carbonate, producing fluorapatite or chlorapatite. It crystallizes in the hexagonal crystal system. Pure hydroxylapatite powder is white. Naturally occurring apatites can, however, also have brown, yellow, or green colorations, comparable to the discolorations of dental fluorosis. Upto 50% of bone by weight is a modified form of hydroxylapatite (known as bone mineral). Carbonated calcium-deficient hydroxylapatite is the main mineral of which dental enamel and dentin are composed. Hydroxylapatite crystals are also found in the small calcifications (within the pineal gland and other structures) known as corpora arenacea or 'brain sand'. (Unqueira, Luiz Carlos *et al*,2003)

Du *et al*. used a biomimetic nano-HA/collagen scaffold with osteogenic cells in organ culture (Du C *et al*,1999). Natural biopolymers such as collagen, fibrin, alginate and hyaluronic acid (Geiger M *et al*,2003), can be used in bone tissue engineering. Synthetic polymers such as poly (a-hydroxyl acids), poly (lactic acid) PLA

Corresponding author: **Prof (Dr.) S.K Biswal**, Mobile No: +91-9438607080

(Mikos AG *et al*,1994), poly (glycolic acid) PGA (Ma PX *et al*,1995) or their co- polymer PLGA (Shea LD *et al*,2000) can also be used as biomaterials for the use in bone tissue engineering.

The development of metal nanoparticles with welldefined shape, size and composition is a big challenge in the field of nanotechnology. Several methods have been reported for the preparation of metal nanoparti- cles (Kometani N *et al*,2001) to control the size (Murphy CJ *et al*,2005) and shape (Sun YG *et al*,2002) of nanoparti- cles. Gold nanoparticles (AuNPs) can be synthesized by the reduction of Chloroauric acid (HAuCl4) using citrate (Misra TK *et al*,2006) sodium borohydride (NaBH4) as reducing agents to synthesize AuNPs in organic solvents (Manna A *et al*,2003). AuNPs can also be prepared by reducing with chitosan in which chitosan acts as a stabilizing agent and a protecting polymer (Esumi K *et al*,2003). But chitosan is having poor solubility in neutral and basic medium; therefore, it is necessary to provide an acidic medium like hydrochloric acid, lactic acid, acetic acid, glutamic acid to dissolve chitosan. (Esumi K *et al*,2003) reported the formation of gold–chitosan nanocomposite by adsorption of chitosan molecules on particle surfaces and evaluated the catalytic activities from elimination of hydroxyl radicals using a spin-trapping technique.

In our laboratory, TSP were modified via carboxymethylation, (Goyal, P *et al*,2007) carbamoylethylation, (Sharma, B. R *et al*,2003) cyanoethylation,18 .Interestingly, there is no work reported on the gold nanoparticles capping with TSP blended with chitosan polymer composite. In the present research program , attempt has been made to synthesize and characterize the gold nanoparticles capping with TSP –Chitosan composite for growth of hydroxyapatite. The nanocomposites were characterized by a number of techniques including Fourier transform infrared spectroscopy (FTIR), scanning electron microscopy (SEM), transmission electron microscopy (TEM), X-ray diffraction (XRD), and electrical conductivity,TGA.

Experimental details

Reagents

Sodium borohydride, Hydrogen tetrachloroaurate (III), 30 wt.% solution in dilute hydrochloric acid, 99.99% was purchased from Sigma-Aldrich St. Louis, MO, USA. Sodium dihydrogen ortho-Phosphate was purchased from Qualigens Fine chemicals, India. Calcium chloride dihydrate extra pure was purchased from Merck Ltd., India. TSP of pharmaceutical grade was used and other chemicals used were of analytical grade. Chitosan was prepared by the modification of earlier methods (Mochizuki *et al*. 1989)

Nanoparticles Synthesis

One gram of TSP was dissolved in 50 mL of double distilled water at 55^{o} C. One gram of Chitosan (C) was dissolved in 50 mL of 0.1 N HCl. To 1 mL of TSP solution, 1 mL of chitosan solution was added and stirred at room temperature till the solution mixture was homogenous (TSP-C). As TSP is soluble in water and could not be precipitated because of its ambiguous isoelectric point chitosan solution was added to the TSP solution (chitosan can be precipitated above pH 6.5 along with TSP). To 2 mL of TSP-C solution, 0.5 mL of aqueous HAuCl4 solution (0.01 M) was added followed by stirring for 1 h. At this time the pH of the solution was around 6. To this resulting solution 0.2 mL of 1 M NaBH4 dissolved in 0.3 M NaOH solution was added drop- wise followed by stirring for 1 h. The solution developed a wine red colour. Later the pH of the solution was brought to 7 using dilute HCl (0.1 N). A fair pink colour was observed which is the characteristic colour of gold nanoparticles. The contents were centrifuged at 6,000 rpm for 15 min; the pellet formed was purified by repeatedly washing with double distilled water to ensure that it was free from any impurities for the preparation of hydroxyapatite. The pellet (TSP-C–Au nanomatrix) was dispersed in 5 mL double distilled water and to this solution 1 mL of CaCl2 solution (1 M) was added followed by addition of 1 mL of NaH_2PO_4 $12H_2O$ solution (1 M), and the contents were stirred for half an hour at room temperature (30 C). The resulting precipitate was centrifuged and washed repeatedly with water. Finally the HAP formed was dried at100^0C for about 5 h. A separate control experiment was conducted as above except that $HAuCl_4$ solution and NaBH4 solution were not added in the reaction mixture

Characterization

XRD

X-ray diffraction (Rigaku, D/Max, 2,500 V, Cu-αa radiation: 1.54056 A °) experiments were carried out on both the plain PAA and the composite samples. Wide-angle X-ray diffractograms were recorded at temperature of 30^0C after isothermal crystallization at this temperature for 1 h.

SEM

Morphology of the Poly(FAn)/c-MWCNTS composite was investigated using a Philip XL 30 SEM at an accelerating voltage of 25 kV. The sample was fractured at liquid nitrogen temperature and then was coated with a thin layer of gold before observation.

TEM

TEM experiments were performed on a Hitachi H-8100 electron microscope with an acceleration voltage of 200 kV.

EDX

Energy-dispersive X-ray spectroscopy (EDX) is an analy-

-tical technique used for the elemental analysis or chemical characterization of a sample. It was recorded in a spot-profile mode by focusing the electron beam onto the specific regions of the sample.

IR Spectra

The Fourier transform infrared (FT-IR) spectra were recorded on a Nicolet 8700 spectrometer, in the range 400–4,000 cm^{-1}.

TGA

TGA studies were performed on a TA instrument (SDT Q600 analyzer) from 30 °C to 800 °C at a heating rate of 10 °C/min under nitrogen atmosphere.

Results and Discussion

As TSP is soluble in water with ambiguous isoelectric point we have prepared TSP–chitosan composite that precipitates at pH around 7. As the backbone of TSP molecule contains carboxylic groups, the calcium ions of the calcium chloride bind to these groups and further calcium ions react with phosphate ions (from NaH_2PO_4) to form a compound like HAP. Addition of chitosan solution to TSP solution is first reported in this article to prepare gold- based HAP nanoparticles.

XRD

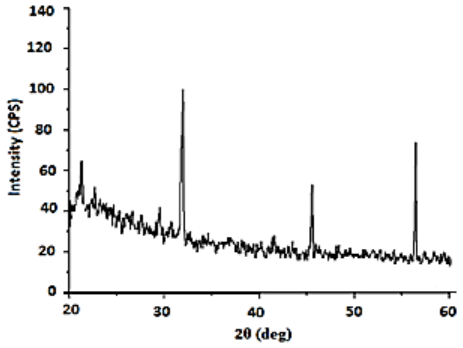

(a)

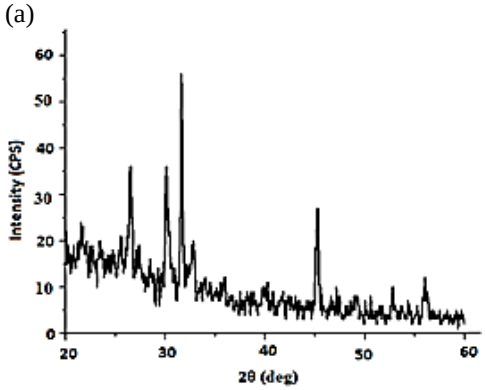

(b)

Fig 1 (a) XRD pattern of GC–Au–HA nanocomposite exhibiting the peaks (b) XRD spectrum of the precipitate obtained in control experiment exhibiting peaks of a-TCP with peaks and b-TCP with peaks at 27.3 and 28.4 apart from HA peaks

Figure 1(a) shows the X-ray diffraction (XRD) pattern of HAP crystals using TSP –chitosan capped gold nanoparticles as a scaffold. The XRD pattern was recorded from a drop-coated sample of HAP on a glass substrate. The peaks at 32.9, 47.4 and 56.6 indicate reflections from 112, 222, 004 crystal planes, respec- tively. These reflections more or less correspond to Bragg reflections of HAP. The result shows that gold nanoparticles induced the formation of HAP nanoparticles on the TSP–chitosan scaffold. Figure 1(b) shows the XRD spectrum of the precipitate formed in the control experiment showing peaks other than HA. These peaks include a-TCP with peaks at 20.6, 24.4 and 26.3, and β-tricalcium phosphate (TCP) with peaks at 27.3 and 28.4 (Park YM *et al*,2008). Without gold nanoparticles it is clear from this results that in the absence of gold nanoparticles, other calcium apatites will form when TSP and Chitosan are used as a medium.

SEM

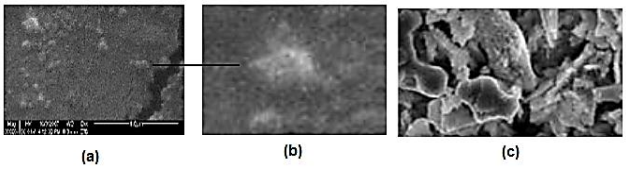

Fig 2 Scanning Electron Microscope image of the GC–Au–HA nanocomposite (a) showing individual crystals with the size in the range 50 to 150 nm (b) and (c) showing aggregated crystals

The surface morphology of the TSP-C–Au capped nanoparticles analysed by scanning electron micro- scope (SEM) is shown in Fig-2 a, b, c. In Fig. 2(a), the size and shape of the individual crystals can be observed. The shape of the crystals is spherical and the sizes of the crystals are in the range of 50 to 150 nm. A beautiful aggregation of these crystals is shown in Fig. 2 (c). The aggregated HA particles exhibited crystalline nature.

TEM

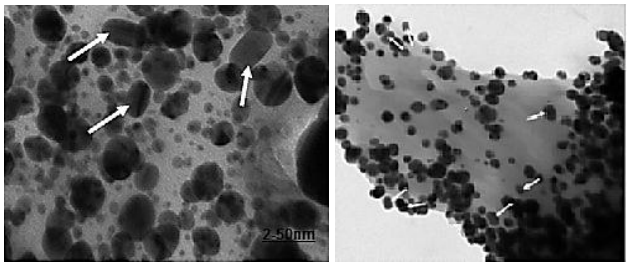

(a) (b)

Fig 3 High Resolution Transmission Electron Microscope images of GC–Au–HA nanocomposite showing the size of nanocomposite (a) 50 nm (b) 5 nm (c) diffraction image of the composite showing the lattice parameters at 004, 112, 222

The High-resolution transmission electron microscopic

(HR-TEM) analysis in Fig. 3(b) has revealed that the size of the nanocomposite formed was in the range of ≥2–50 nm. The aggregations of these nanoparticles are represented in Fig. 3(a). The selected area of diffraction. HA shows the Bragg deflections at 004, 112, 222. These studies have confirmed the nanosized components of TSP-C–Au– HA nanocomposite.

EDX Spectrum

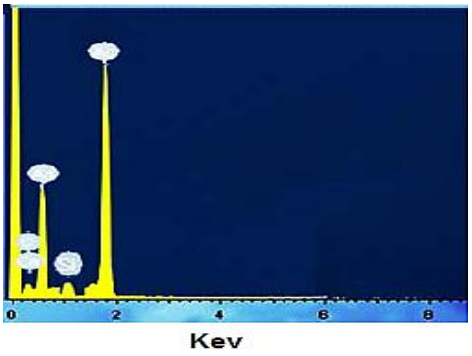

Fig 4 EDX profile showing the Ca and P signals of TSP-C–Au– HA nanocomposite

The Energy dispersive spectroscopy (EDX) spectrum of the nanocomposite formed is shown in fig. 4. The calcium and phosphorus signals are very clearly seen indicating the formation of calcium phosphates. The ratio of Ca to P was found to be 1.64:1 and the value is similar with that of synthetic HA.

FTIR

The structure of the chitosan biocomposite particles was analyzed by using FTIR spectroscopy. Figure 5 (a) shows FTIR spectra of TSP/chitosan biocomposites. A characteristic band at 3450 cm^{-1} is attributed to $–NH_2$ and –OH groups stretching vibration and the band for amide I at 1655 cm^{-1} is seen in Fig. which is the infrared spectrum of chitosan. Peaks at 1612 cm^{-1} (N–H bending),1566 cm^{-1} (N–H bending), 1450 and 1425 cm^{-1} (C–H bending), and also absorbencies due to structural O–H stretching at 3450 cm^{-1} , H–O–H deforming (absorbed water) at 1655 cm^{-1} , and **fig- 5 (b)** a band at 1648 cm $^{-1}$ is attributed to the absorption band of the carbonyl (-HC=O) stretching . It

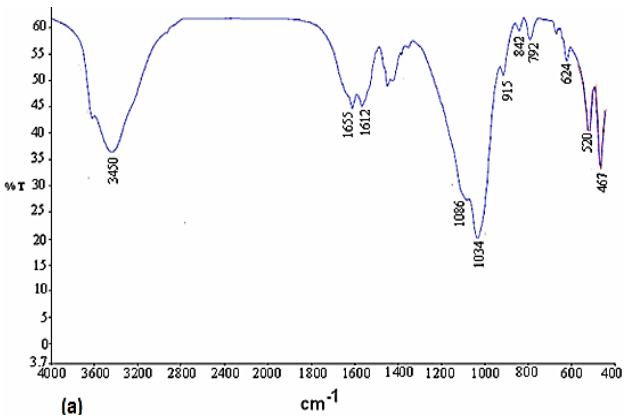

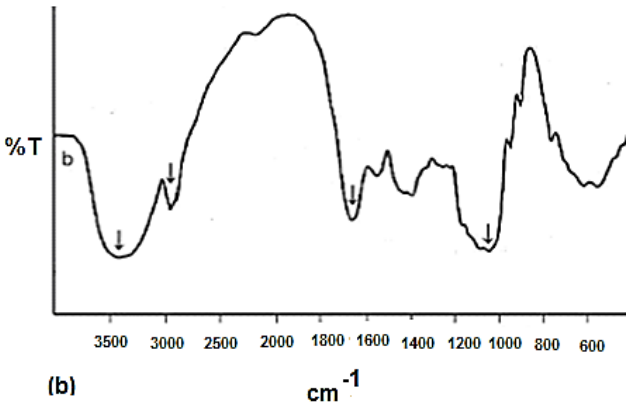

Fig 5 FTIR of the TSP-C–Au–HA nanocomposite showing the phosphate vibrational modes of v_1, v_2, v_4 of HA. (b) FTIR of the precipitate obtained in control experiment

may be explained by the fact that each monosaccharide of tamarind gum has two isomers, comprising of a ring system and a chain system, which results in the appearance of the carbonyl absorption band. The other band at 1041 cm $^{-1}$ that was assigned to the stretching vibration of (CH-OH) appeared at 1643 cm^{-1} and other peaks that is -OH group present at 3400 cm^{-1} and peak attributed to the –CH2 group present 2926 cm^{-1} .

TGA

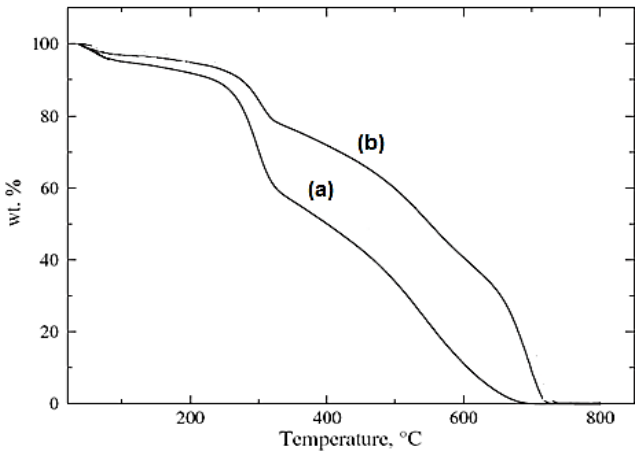

Fig 6 Thermogram of the TSP-C–Au–HA nanocomposite exhibiting the two stage weight loss due to the decomposition of TSP and Chitosan. (b) Thermogram of the precipitate obtained in control experiment

The thermogram of TSP-C–Au–HA nanocomposite is shown in Fig. 6a. The composite loses its moisture and the bound water up to 199 ^{0}C. Approximately 5% protein loss was observed between 199 and 429 ^{0}C which is due to the degradation of TSP. Around 11% loss was observed between 429 and 825^{0}C which was attributed to further degradation of the material or evolution of CO_2. The remaining 74% of the inorganic material is considered as HA, whereas the thermogram of the precipitate obtained in the control experiment (Fig. 6b) shows 62% of the inorganic material at 785^{0}C. About 12% more inorganic

material formed in the experiment using gold nanoparticles indicates a better yield.

Conclusions

It is evident from the study that TSP–chitosan capped gold nanoparticles can act as a matrix for the growth of HAp crystals. We were able to produce HAp nanoparticles on the surface of TSP–chitosan capped gold nanoparticles in this study. This method is cost-effective with a yield of 74% nano-HA.

Reference

G. Cao (2004), Nanostructures and Nanomaterials, *Imperial College Press*, London.

M. A. Reed and T. Lee (2003), Molecular Nanoelectronics, *American Scientific, Stevenson Ranch*, Calif, USA.

C. P. Poole and F. J. Owens (2003), Introduction to Nanotechnology, *Wiley Interscience*, New York, NY, USA.

A. Taleb, C. Petit, and M. P. Pileni (1998), Optical properties of selfassembled 2D and 3D superlattices of silver nanoparticles, *Journal of Physical Chemistry B*, vol. 102, no. 12, pp. 2214–2220.

M. A. Noginov, G. Zhu, M. Bahoura *et al*.(2006), The effect of gain and absorption on surface plasmons in metal nanoparticles, *Applied Physics B*, vol. 86, no. 3, pp. 455–460.

C. S. Onnichsen, T. Franzl, T. Wilk, G. Von Plessen, and J. Feldmann (2002), Plasmon resonances in large noble-metal clusters, *New Journal of Physics*, vol. 4, pp. 93.1–93.8.

Zhao F, Yin YJ, Lu WW, Leong JC, Zhang WJ, Zhang JY, Zhang MF, Yao KD (2002), Preparation and histological evaluation of biomimetic three-dimensional hydroxyapatite/ chitosan–gelatin network composite scaffolds, *Biomaterials*, 23:3227–3234

Suh JKF, Matthew HWT (2000), Application of chitosan-based polysaccharide biomaterials in cartilage tissue engineering: a review, *Biomaterials*, 21:2589–2598

Khor E, Lim LY (2003), Implantable applications of chitin and chitosan, *Biomaterials*, 24:2339–2349

Dufresne A, Cavaille JY, Dupeyre D, Garcia-Ramirez M, Romero J (1999), Morphology, phase continuity and mechanical behaviour of polyamide 6 chitosan blends, *Polymer* ,40:1657–1666

Mao JS, Zhao LG, Yin YJ, Yao KD (2003), Structure and properties of bilayer chitosan–gelatin scaffolds, *Biomaterials*, 24:1067–1074

Gurpreet Kaur, Subheet Jain, and Ashok K. Tiwary (2010), Chitosan-Carboxymethyl Tamarind Kernel Powder Interpolymer Complexation: *Investigations for Colon Drug Delivery Sci Pharm*. 2010 March 30; 78(1): 57–78. Published online 2009 December 3. doi: 10.3797/scipharm.0908-10

Unqueira, Luiz Carlos; José Carneiro (2003), Foltin, Janet; Lebowitz, Harriet; Boyle, Peter J.eds. Basic Histology, Text & Atlas (10th ed.). McGraw-Hill Companies. p. 144. ISBN 0-07-137829-4. Inorganic matter represents about 50% of the dry weight of bone crystals show imperfections and are not identical to the hydroxylapatite found in the rock minerals

Du C, Cui FZ, Zhu XD, de Groot K (1999), Three-dimensional nano-HAp/collagen matrix loading with osteogenic cells in organ culture, *J Biomed Mater Res*, 44:407–415

Geiger M, Li RH, Friess W (2003), Collagen sponges for bone regeneration with rhBMP-2, *Adv Drug Deliv Rev*, 55:1613–1629

Mikos AG, Thorsen AJ, Czerwonka LA, Bao Y, Langer R, Winslow DN, Vacanti JP (1994), Preparation and characterization of poly(L-lactic acid) foams, *Polymer*, 35:1068–1077

Ma PX, Langer R (1995), In: Mikos AG *et al* (eds) Polymers in medicine and pharmacy, *MRS, Pittsburgh*, pp 99–104

Shea LD, Wang D, Franceschi RT, Mooney DJ (2000), Engineered bone development from a pre-osteoblast cell line on three-dimensional scaffolds, *Tissue Eng* 6:605–617

Kometani N, Tsubonishi M, Fujita T, Asami K, Yonezawa Y (2001), Preparation and optical absorption spectra of dyecoated Au, Ag, and Au/Ag colloidal nanoparticles in aqueous solutions and in alternate assemblies, *Langmuir*, 17:578–580

Murphy CJ, San TK, Gole AM, Orendorff CJ, Gao JX, Gou L, Hunyadi SE, Li T (2005), Anisotropic metal nanoparticles: synthesis, assembly, and optical applications, *J Phys Chem B*,109:13857–13870

Sun YG, Xia YN (2002), Shape-controlled synthesis of gold and silver nanoparticles, *Science*, 298:2176–2179

Misra TK, Chen TS, Liu CY (2006), Phase transfer of gold nanoparticles from aqueous to organic solution containing resorcinarene, *J Colloid Interface Sci*, 297:584–58

Manna A, Chen PL, Akiyama H, Wei TX, Tamada K, Knoll W (2003), Optimized photoisomerization on gold nanoparticles capped by unsymmetrical azobenzene disulfides, *Chem Mater*, 15:20–28

Esumi K, Takei N, Yoshimura T (2003), Antioxidant-potentiality of gold–chitosan nanocomposites, *Colloids Surf B Biointerfaces*, 32:117–123

Sharma, B. R.; Kumar, V.; Soni, P. L.; Sharma, P. (2003), *J Appl Polym Sci*, 89, 3216–3219.

Goyal, P.; Kumar, V.; Sharma, P.(2007), Carbohydr Polym, 69, 251–255.

Sharma, B. R.; Kumar, V.; Soni, P. L.(2003), Carbohydr Polym 54, 143–147.

Sharma, B. R.; Kumar, V.; Soni, P. L.(2004), Carbohydr Polym,58, 449–453.

Park YM, Ryu SC, Yoon SY, Stevens R, Park HC (2008), Preparation of whisker-shaped hydroxyapatite/b-tricalcium phosphate composite, *Mater Chem Phys*, doi: 10.1016/j.matchemphys.2007.12.013